SCIENTIFIC REPORTS

OPEN

SUBJECT AREAS:
CHEMISTRY
MATERIALS SCIENCE

Received
19 December 2013

Accepted
23 January 2014

Published
7 February 2014

Correspondence and requests for materials should be addressed to R.D. (renaud.demadrille@cea.fr) or E.P. (epalomares@ICIQ.ES)

A Robust Organic Dye for Dye Sensitized Solar Cells Based on Iodine/Iodide Electrolytes Combining High Efficiency and Outstanding Stability

Damien Joly[1], Laia Pellejà[2], Stéphanie Narbey[3], Frédéric Oswald[3], Julien Chiron[4], John N. Clifford[2], Emilio Palomares[2,5] & Renaud Demadrille[1]

[1]INAC/SPrAM UMR 5819 (CEA-CNRS-U.J.F-Grenoble 1) 17 Rue des Martyrs, 38054 Grenoble Cedex 9, France, [2]Institute of Chemical Research of Catalonia (ICIQ). Avda. Països Catalans, 16. Tarragona. E-43007. Spain, [3]Solaronix SA, Rue de l'Ouriette 129, 1170 Aubonne, Switzerland, [4]KaïronKem, 20 rue Marc Donadille, Technopôle Chateau Gombert, 13013 Marseille, France, [5]ICREA. Passeig Lluís Companys, 23. Barcelona. E-08010. Spain.

Among the new photovoltaic technologies, the Dye-Sensitized Solar Cell (DSC) is becoming a realistic approach towards energy markets such as BIPV (Building Integrated PhotoVoltaics). In order to improve the performances of DSCs and to increase their commercial attractiveness, cheap, colourful, stable and highly efficient ruthenium-free dyes must be developed. Here we report the synthesis and complete characterization of a new purely organic sensitizer (RK1) that can be prepared and synthetically upscaled rapidly. Solar cells containing this orange dye show a power conversion efficiency of 10.2% under standard conditions (AM 1.5G, 1000 Wm^{-2}) using iodine/iodide as the electrolyte redox shuttle in the electrolyte, which is among the few examples of DSC using an organic dyes and iodine/iodide red/ox pair to overcome the 10% efficiency barrier. We demonstrate that the combination of this dye with an ionic liquid electrolyte allows the fabrication of solar cells that show power conversion efficiencies of up to 7.36% that are highly stable with no measurable degradation of initial performances after 2200 h of light soaking at 65°C under standard irradiation conditions. RK1 achieves one of the best output power conversion efficiencies for a solar cell based on the iodine/iodide electrolyte, combining high efficiency and outstanding stability.

Dye Sensitized Solar Cells (DSCs) are attracting much attention because of their relatively high conversion efficiencies, low cost production processes and short energy payback time[1]. In these devices, sunlight is absorbed by photoactive molecules that are attached to the surface of a wide band gap semiconductor oxide (typically TiO_2 or ZnO) forming a dense monolayer. The system is completed using a hole transporting material which is usually a liquid electrolyte containing the iodide/tri-iodide (I^-/I_3^-) red/ox couple[2]. The molecules act as sensitizers and upon photo-excitation inject an electron into the conduction band of the metal oxide. While the electrons are conducted through the nanostructured metal oxide to reach the external circuit, the oxidized dye is regenerated by the red/ox couple, which is itself regenerated at the counter electrode[3,4]. The complete description of the basic working principles of a DSC can be found elsewhere[5,6].

Several different classes of materials are employed to fabricate a DSC, but the sensitizer is probably the key element since it governs the photon harvesting and the creation of free charges after injection of electrons into the nanostructured semi-conducting oxide. Moreover, the sensitizer structure has also been shown to control key electron transfer processes at the TiO_2/dye/electrolyte interface such as the recombination of TiO_2 electrons with electrolyte species or with dye cations themselves. For this reason many efforts have recently focused on the development of new efficient sensitizers that could help improve device performance and allow for practical and real use of this technology beyond the laboratory.

For many years, ruthenium based complexes were the "champion" dyes of DSCs and some of them were distinguished by achieving more than 11% efficiency[7]. However, despite the fact that high power conversion efficiencies and relatively stable DSCs have been fabricated using ruthenium sensitizers, Ruthenium cannot be considered an "earth abundant material" and, thus, it is desirable to look for alternative dyes. Besides, even though some ruthenium complexes show broad absorption spectra, they generally have modest molar extinction coefficients[8,9] whichs limit

their performances when employed to sensitize thin electrodes. As a consequence, this class of sensitizer is not ideal for DSCs based on ionic-liquids as thin electrodes are preferable due to the high inherent viscosity of these electrolytes[10].

To overcome this problem, the use of organic sensitizers has been demonstrated to be a useful strategy. Organic sensitizers have attracted great interest because of their potentially lower production costs, easier and more versatile synthesis, and much larger molar absorption coefficients. In addition, some of them have shown satisfactory stability[11,12]. Many different organic dyes with conversion efficiencies in the range of 6–8% have been reported in the last years but only a few examples have overcome efficiencies of 10%[13–16]. To date, the highest efficiency for a DSC employing a purely organic sensitizer has been achieved by Wang and co-workers using an electrolyte based on iodide/tri-iodide in a volatile electrolyte. Using C219, a high absorbing dye prepared in ten steps, they reported 10.1% power conversion efficiency under 1 Sun irradiation[17].

In addition to purely organic dyes, metallated porphyrins showing strong absorption in the visible region, have been synthesized and tested in DSCs by Grätzel and co-workers[18]. After appropriate tailoring of the chemical structure and employment of a cobalt electrolyte, the porphyrin dye YD2-*o*-C8 showed power conversion efficiencies of up to 11.9% under standard conditions (AM 1.5 G, 100 $mWcm^{-2}$ intensity) which was further improved to 12.3% when co-sensitized with an organic dye[19]. However, porphyrins usually require complicated synthetic strategies with relatively low yields, especially when an anchoring function and a redox group have to be introduced at specific positions[20]. For this reason, our motivation in this work was to design a simple, easy to prepare and efficient organic sensitizer. Our strategy was principally driven by the possibility to reduce the number of chemical steps involved in its preparation, the availability of the organic precursors and the possibility to confer to the dye tailored optical and electrochemical properties. In the literature, most of the new organic sensitizers are prepared using the very well-known donor-π-acceptor design approach, where the donor bears alkyls chains and the π conjugated bridge is mainly based on symmetrical chromophoric units. Our approach, on the other hand, is based on the use of a dissymmetric π-conjugated bridge that embeds an alkyls chain and an electro deficient unit localized close to the electron-withdrawing anchoring function and an electron-rich unit close to the aryl amine donating group[21,22]. The introduction of a phenyl ring between acceptor benzothiadiazole (BTD) and the cyanoacrylic acid group should stabilize the dye radical cation and decrease recombination rate as showed by Haid et al.[23].

Herein we report the preparation of a new purely organic dye, **RK1**, whose synthesis involves just five steps which starts from low cost precursors, resulting in a solar to electrical power conversion efficiency of 10.2% under standard conditions (AM 1.5 G, 100 $mWcm^{-2}$ intensity). To the best of our knowledge, this represents one of the best power conversion efficiencies ever reported for a DSC based on a purely organic dye. Moreover, this high efficiency is coupled with outstanding long-term stability as demonstrated by devices based on an ionic liquid electrolyte.

Results

RK1 synthesis. The chemical structure of **RK1** is shown in Scheme 1. The thiophene BTD phenyl chromophore constitutes the π bridge in this D–π–A structure. **RK1** has a very simple chemical structure, and its preparation does not require complicated synthetic procedures or purification steps allowing for its preparation in the tens of grams scale.

The convergent synthetic strategy to access **RK1** relies on the preparation of two key building blocks (1 and 2) that are subsequently coupled together via a Suzuki or a Stille cross coupling reaction (see Figure 1). The preparation of these two intermediates is based on the use of low cost and commercially available precursors and a classical palladium cross coupling reaction. With the idea in mind of potential future synthesis of this dye at an industrial level, toxic reaction solvents such as DMF were purposely not used in our synthetic scheme. In addition, the replacement of DMF by a mixture of toluene, THF and water helped us to strongly improve the yields of the Suzuki coupling reaction. The overall yield of preparation for **RK1** is 50% after just five steps.

Optical and electrochemical data. The optical properties of the dye were investigated by UV-Visible spectroscopy in ethanol solution and compared to those of N719 which was used as a reference compound in this study (Figure 2 and Table 1). The UV-Vis spectrum of **RK1** shows, as expected, two absorption bands between 300 and 580 nm. The first one which is located in the UV region (λ = 366 nm, ε = 45000 $M^{-1}.cm^{-1}$) is assigned to the π-π* transition of the aromatic rings, whereas the second absorption band

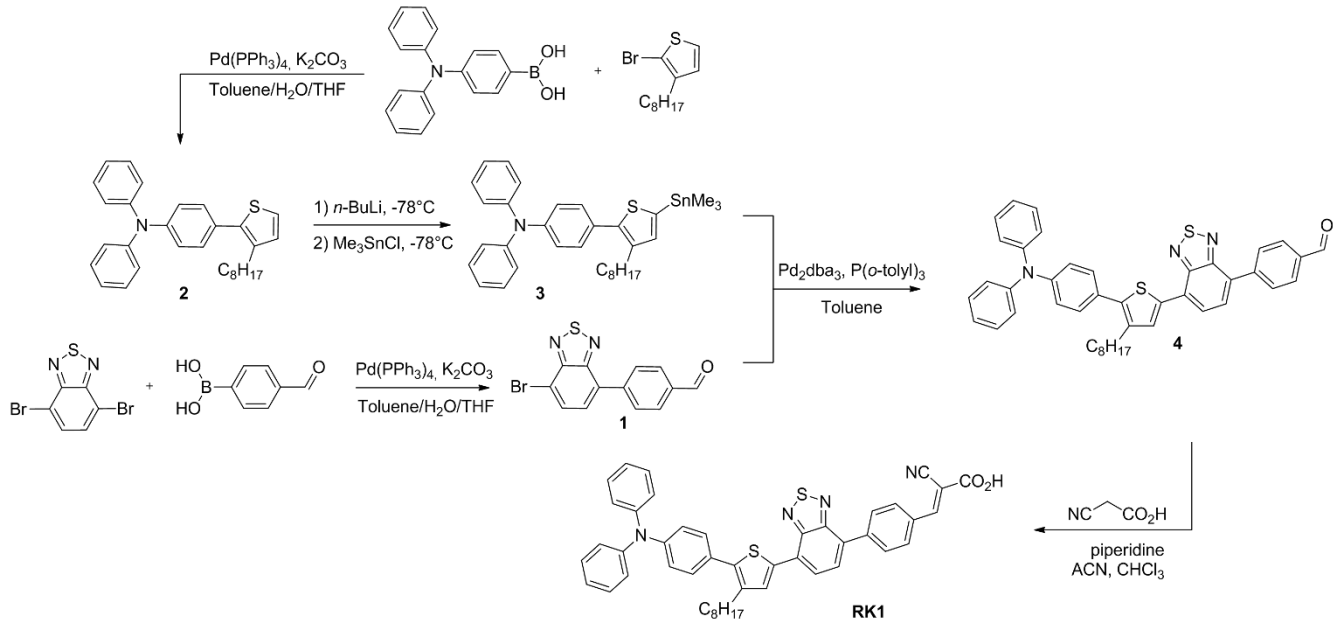

Figure 1 | Synthetic route and reaction conditions for the preparation of RK1.

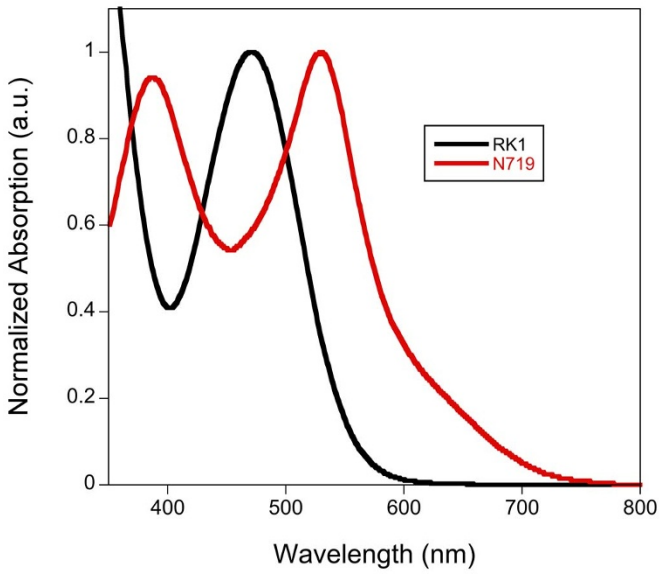

Figure 2 | **UV-Visible absorption spectra of RK1 and N719 in ethanol solution.**

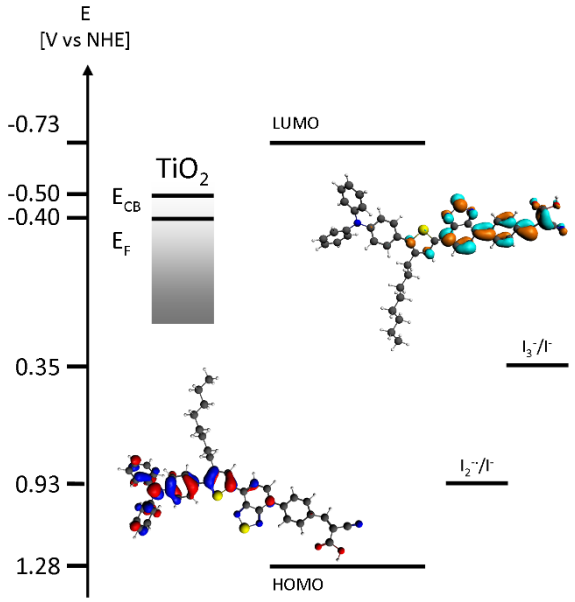

Figure 3 | **Frontier molecular orbitals of RK1 calculated at B3LYP level of theory.**

in the visible region ($\lambda = 470$ nm, $\varepsilon = 26600$ $M^{-1}.cm^{-1}$) is attributed to the internal charge transfer (ICT) transition that occurs between the electron-withdrawing and electron-donating segments of the molecule. This band is at shorter wavelength with respect to that of N719 but the measured molar extinction coefficient at 470 nm for **RK1** is almost two times higher than the corresponding values for N719. As a consequence, **RK1** shows an aesthetically pleasing orange colour both in solution and on TiO_2 films.

The electrochemical properties of **RK1** were investigated by cyclic voltammetry (CV) with the goal to determine the energy level positions of frontier orbitals. Upon the application of negative potentials, the dye undergoes a quasi-reversible reduction/re-oxidation process, and upon the application of positive potentials it showed two reversible oxidation waves corresponding to an oxidation/re-reduction process. The first oxidation peak (*Eox1*) was found at 0.98 V versus NHE which can be assigned to the oxidation of the triphenylamine donor moiety. The second oxidation potential (*Eox2*) was observed at 1.41 V and is attributed to the oxidation of the π-conjugated backbone. The HOMO and LUMO energy level positions determined from the onset of the first oxidation and reduction potential were 0.93 and −0.72 V vs. NHE. **RK1** therefore showed a bandgap (Eg_{CV}) of 1.65 eV. The experimentally determined LUMO energy level of **RK1** lies above the conduction band edge of TiO_2 (0.40 V versus NHE), which ensures the necessary driving force for electron injection from the dye into the conduction band of the semiconductor. Moreover, the HOMO energy level positioned at 0.93 V versus NHE also indicates that there is a sufficient energy offset for regeneration by the I^-/I_3^- redox couple at −0.35 V versus NHE[24].

In order to compare these experimental values and to gain insight into structural properties, the electron density distribution of the frontier orbitals of **RK1** was determined by density functional theory (DFT) using the B3LYP hybrid functional (see Experimental Section for details). We report in Figure 3 the calculated molecular orbital energy diagram for **RK1**, along with *iso* density plots of the HOMO and LUMO. The dyes show a directional electron distribution, with the delocalization of the HOMO on the triphenylamine group and the thiophene of the π-conjugated bridge. On the other hand, the LUMO is predominantly delocalized on the BTD-phenylvinylcyanoacetic units. This directional electron distribution is consistent with the dissymmetrisation of the core and should facilitate the reduction of the oxidized dyes by the I^-/I_3^- based electrolyte, and the injection of electrons into the conduction band of TiO_2.

Dye sensitized solar cells. *Solar cells with liquid electrolyte*. The photovoltaic parameters of the best **RK1** DSCs using a standard acetonitrile based electrolyte are shown in Table 2 alongside those for a device made using the ruthenium sensitizer N719 for comparison. The photoactive electrodes of these devices were fabricated using standard double layer structure consisting of mesoporous TiO_2 and a TiO_2 scatter layer. The I-V curves of champion cells recorded under AM 1.5, 1 Sun illumination and in the dark and their photocurrent response (IPCE) are shown in Figure 4. It should be underlined that the results presented here

Table 1 | Optical and electrochemical data of RK1

	λ_{abs}[a] [nm]	ε[a] [M^{-1}/cm]	Eg_{opt}[b] [eV]	Eox1[c] [V vs NHE]	Eox2[c] [V vs NHE]	Ered[c] [V vs NHE]	HOMO[d] [V vs NHE]	LUMO[d] [V vs NHE]	Eg_{cv}[e] [eV]
RK1	366 470	45000 26600	2.17	0.98	1.41	−0.74	0.93	−0.72	1.65

[a]Measured in Ethanol.
[b]measured from λ_{onset}.
[c]All potentials were obtained during cyclic voltammetric investigations in 0.2 M Bu_4NPF_6 in CH_2Cl_2. Platinum electrode diameter 1 mm, sweep rate: 200 mV s^{-1}. Potentials measured vs Fc^+/Fc were converted to NHE by addition of +0.69 V.
[d]Determined from oxidation onset and reduction onset.
[e]Calculated Eg_{cv} = HOMO-LUMO.

Table 2 | Photovoltaic parameters of DSCs employing an acetonitrile electrolyte

Adsorbing Solution	TiO_2 Thickness [μm]	J_{sc} [mA.cm^{-2}]	V_{oc} [V]	FF [%]	η [%]
RK1 (0.2 mM)/Cheno (10 mM)[a]	4 + 3.5[c]	12.44	0.744	76	7.07
RK1 (0.2 mM)/Cheno (10 mM)[a]	8 + 3.5[c]	13.60	0.719	76	7.50
RK1 (0.2 mM) without Cheno[b]	13 + 3.5[c]	20.25	0.691	64	8.89
RK1 (0.2 mM)/Cheno (2 mM)[b]	13 + 3.5[c]	20.25	0.715	68	9.89
RK1 (0.2 mM)/Cheno (4 mM)[b]	13 + 3.5[c]	19.45	0.704	66	8.98
RK1 (0.2 mM)/Cheno (2 mM)[b]	3.5 + 6.5 + 3.5[d]	18.33	0.734	71	9.52
RK1 (0.2 mM)/Cheno (2 mM)[b]	3.5 + 9.5 + 3.5[d]	19.50	0,713	72	10.00
RK1 (0.5 mM)/Cheno (5 mM)[a]	13 + 4[e]	18.26	0.760	74	10.20
N719 (0.5 mM)/Cheno (5 mM)[a]	13 +4[e]	17.91	0.800	71	10.19

[a]in ethanol.
[b]in methanol.
[c]TiO_2 Solaronix (HT/SP + R/SP), measurements were carried out with a mask of 0.36 cm^2.
[d]TiO_2 macrochannel Solaronix (HT/SP + MC/SP + R/SP), measurements were carried out with a mask of 0.36 cm^2.
[e]TiO_2 Dyesol (18NR-T + 18NR-AO), measurements were carried out with a mask of 0.16 cm^2.

were reproduced in two different laboratories (ICIQ and Solaronix) and that three different cells were fabricated for each entry of the table.

In order to investigate and optimize the DSC performances of the new dye, the TiO_2 film thickness was varied between 4 and 13 μm onto which a 3.5 to 4 μm scattering layer was deposited. For the dyeing of the TiO_2 electrodes, 0.2 to 0.5 mM solutions of **RK1** containing various amounts of 3α, 7α-dihydroxy-5β-cholic acid (chenodeoxycholic acid) were employed. Though the use of chenodeoxycholic acid with organic sensitizers is known to reduce the sensitizer's loading, it has also been shown to diminish the undesirable formation of dye aggregates on the TiO_2 surface and decrease recombination processes between TiO_2 electrons and electrolyte species[25].

Interestingly for **RK1** devices performances remain higher than 7% even for low TiO_2 film thicknesses. When thicker electrodes (10 to 13 μm) are employed, very high current densities of up to 20.25 mA/cm^2 can be attained. This results in a power conversion efficiency of 10.2% for the **RK1** champion cell which is outstanding for an organic sensitizer.

The J_{sc}, FF and V_{oc} for champion cells of **N719** and **RK1** with power conversion efficiencies of over 10%, are rather similar. The dark current in both devices is nearly identical. The photocurrent response (IPCE) shows that though the N719 device performs better at longer wavelengths, **RK1** performs significantly better at shorter wavelengths, in agreement with the respective absorption spectra of these dyes (Figure 2).

The Voc of a DSC is determined by the quasi-Fermi-level of the metal oxide semiconductor, which is correlated with its conduction band edge (Ec) and electron density. Electron density is itself dependent on rate of recombination between semiconductor electrons and oxidized electrolyte species. To investigate the difference in voltage for these devices, charge extraction and transient photovoltage measurements were conducted. Charge extraction data (Figure 5(a)) show that the **RK1** device has a slightly higher charge density with respect to the N719. This indicates that the TiO_2 conduction band in **RK1** devices is shifted downward somewhat compared to N719 devices. Electron lifetime measured using transient photovoltage measurements (Figure 5(b)) for the **RK1** device is shorter than for the N719 device. This is routinely observed for DSCs employing organic sensitizers[26]. Therefore, the combined effect of the lower lying TiO_2 conduction band and shorter electron lifetime explains the general trend of lower V_{oc} for **RK1** devices.

Solar cells with ionic liquid electrolyte. For the practical application of dye-sensitized solar cells (DSCs), in addition to high performances, long device lifetime is a major requirement. Because highly volatile solvents such as acetonitrile are inappropriate for stability measurements, a solvent-free ionic liquid electrolyte was used instead in order to evaluate the lifetime of the **RK1** sensitizer under thermal stress and light soaking. The photovoltaic parameters of these solar cells are given in Table 3. Two different types of electrodes were used

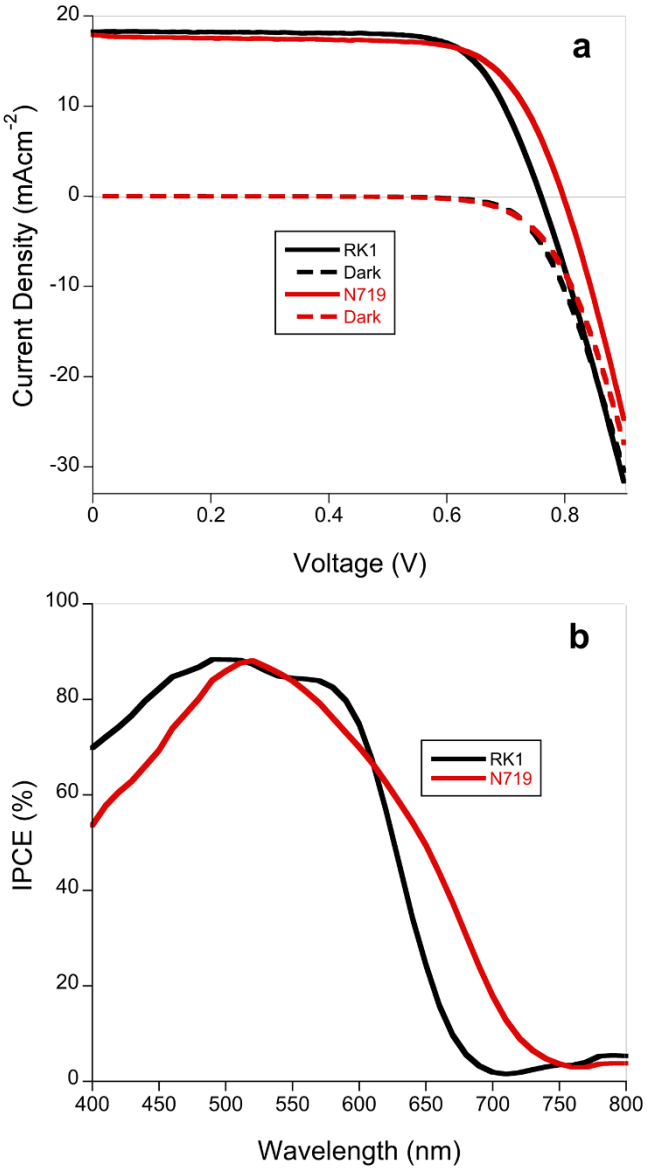

Figure 4 | (a) I-V curves recorded under AM 1.5 illumination and in the dark and (b) IPCE spectra for RK1 **and N719 devices.**

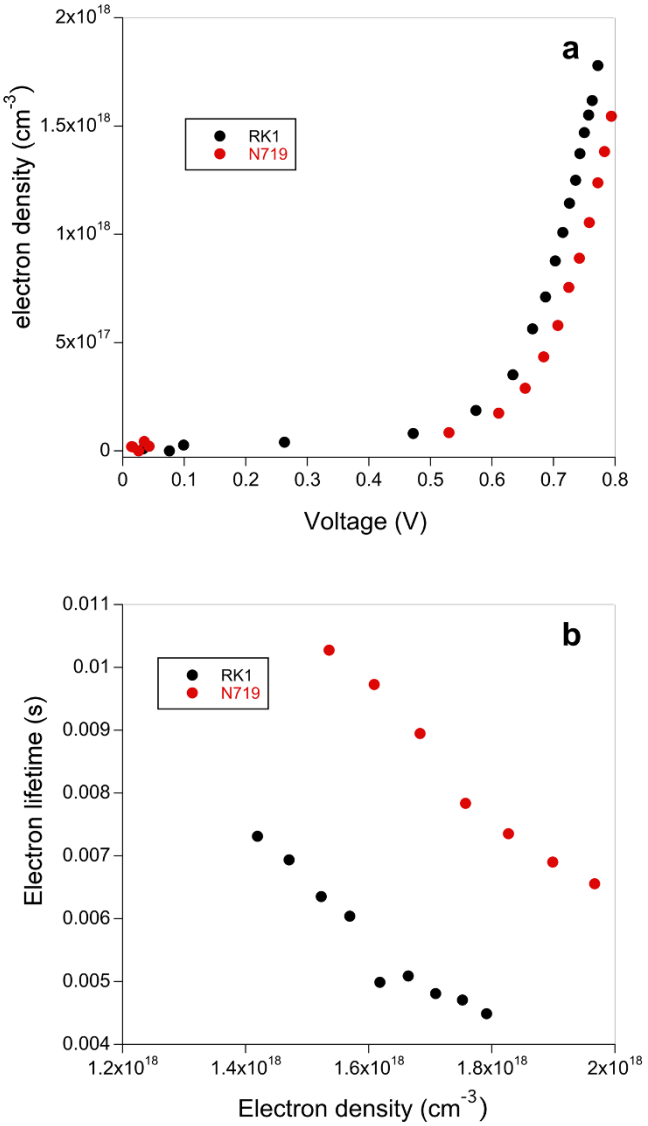

Figure 5 | (a) Charge extraction data showing electron density as a function of induced voltage and (b) transient photovoltage data showing electron lifetimes versus electron density for N719 and RK1 DSC devices.

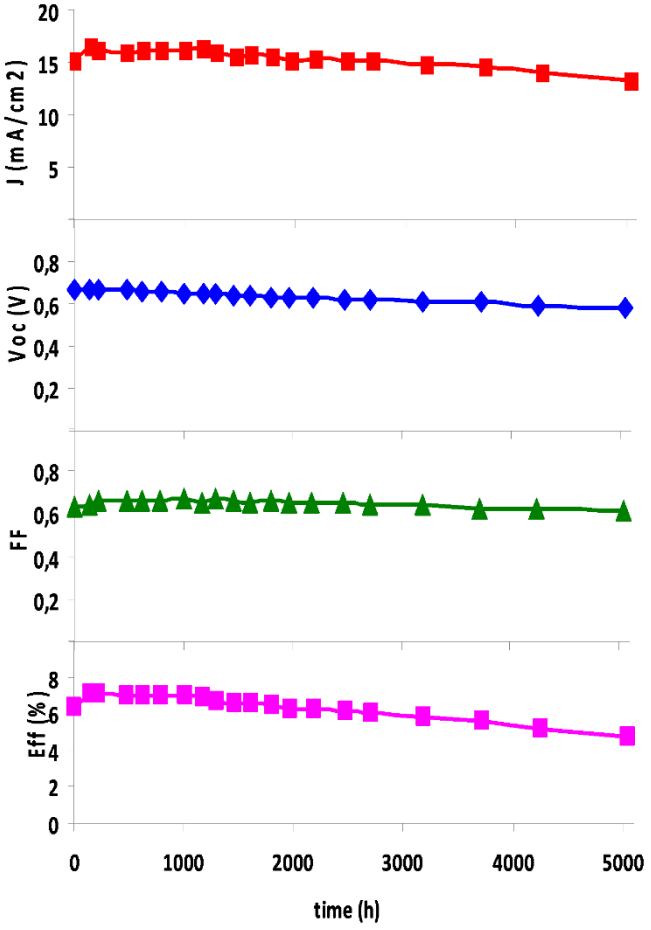

Figure 6 | Detailed photovoltaic parameters of a cell measured under the irradiance of AM 1.5 G sunlight during successive full-sun visible-light soaking (1 sun 1000 W/m^2) at 65°C. Jsc: short-circuit photocurrent density; Voc: open-circuit voltage; FF: fill factor; η: power conversion efficiency.

to fabricate the devices. In addition to regular mesoporous TiO_2, to further increase the thickness of the electrode, a macro channel TiO_2 paste was employed. This strategy was found to be particularly efficient to improve the light-harvesting capacity of these devices without alteration of the capability of the viscous ionic liquid electrolyte to penetrate deeply into the nanostructured electrode. With 8 µm thick TiO_2 film coated with a 3.5 µm thick reflecting layer, devices showing a J_{sc} of 15.40 mA/cm^2, a V_{oc} of 0.665 V, a FF of 69% and a power conversion efficiency of 7.36% at 1 Sun were obtained. This performance ranks among the best reported for organic sensitizers using ionic liquid electrolyte and is considerably better than most of the performances reported for Ruthenium based dyes[27,28]. The fabricated DSCs were irradiated continuously in a solar simulator with a light intensity of 1000 W/cm^{-2} at 65°C. The evolution of the photovoltaic parameters of a cell measured under the irradiance of AM 1.5 G sunlight during successive full-sun visible-light soaking is presented in Figure 6. After light soaking, the power conversion efficiency of the solar cell significantly increases; this behaviour is related to the improved penetration of the ionic liquid electrolyte through the complete thickness of the electrode and the "activation" of the entire electrode[29]. After this period we observed a stabilisation of the performances and no degradation; this cell exhibits outstanding

Table 3 | Photovoltaic parameters of DSCs with an ionic liquid electrolyte

Adsorbing Solution	TiO_2 Thickness [µm]	J_{sc} [mA.cm^{-2}]	V_{oc} [V]	FF [%]	η [%]
RK1 (0.2 mM)/Cheno (10 mM)[a]	4 + 3.5[c]	12.22	0,684	72	6.04
RK1 (0.2 mM)/Cheno (2 mM)[a]	6 + 3.5[c]	13.70	0,671	66	6.06
RK1 (0.2 mM)/Cheno (2 mM)[b]	4 + 4 + 3.5[d]	15.40	0.665	69	7.36

[a]in Ethanol.
[b]in Methanol.
[c]TiO_2 Solaronix (HT/SP + R/SP).
[d]TiO_2 macrochannel Solaronix (HT/SP + MC/SP + R/SP), all measurements were carried out with a mask of 0.36 cm^2.

stability with no measurable degradation of the initial performances after 2200 h of irradiation. After this period the cells start to undergo a linear degradation of their performances but it is noteworthy that after 5000 h continuous irradiation at 65°C, the degraded solar cells still show 75% of their initial power conversion efficiency. From the best of our knowledge this stability performance is the best ever achieved for an organic sensitizer.

Discussion

We have designed and synthesized a novel donor-acceptor organic dye (**RK1**) based on a dissymmetric central core embedding a benzothiadiazole chromophoric unit. This dye has a simple chemical structure and can be prepared very easily in five steps with an overall yield of 50%. When employed in DSCs with liquid electrolytes containing the I^-/I_3^- redox couple, under standard conditions a high short circuit current of 18.26 mA/cm^2, an open circuit voltage of 0.76 V and a FF of 74% were achieved leading to an overall power conversion efficiency of 10.2%. This represents one of the highest efficiencies ever recorded for a DSC device employing a fully organic dye and iodine/iodide electrolytes. In addition, when a solvent-free ionic liquid electrolyte was used a short circuit current of 15.40 mA/cm^2, an open circuit voltage of 0.665 V and a FF of 69% leading to a power conversion efficiency of 7.36% under standard conditions was achieved. These DSC devices showed outstanding stability when irradiated continuously with 1000 W/cm^{-2} light intensity at 65°C with no measurable degradation of the initial performances after 2200 h and only a loss of circa 25% after 5000 h. We note that these results are obtained with iodide/tri-iodide that has a strong absorption band located at 360 nm[30] and that the photocurrent generated by the sensitizer could be further improved in the blue part of the spectrum with the replacement of this electrolyte by a cobalt redox shuttle. In addition, such redox shuttles can be used to increase Voc further improving device performance. To conclude, we believe that **RK1** is a most promising organic dye for future low cost, stable and efficient dye sensitized solar cells.

Methods

Materials synthesis. 2-bromo-3-octylthiophene, 4-(N,N-diphenylamine) phenylboronic acid, 4-formylphenyl-boronic acid, 2-cyanoacetic acid, piperidine, *n*-BuLi [2.5 M solution in Tetrahydrofuran (THF)], trimethyl tin chloride solution [1 M solution in *n*-hexane] were purchased from Aldrich or TCI chemicals and used as received. N-Bromo-Succinimide (NBS) was purchased from Fisher Chemicals and 4,7-dibromo-2,1,3-benzothiadiazole from Orgalight or provided by Kaïronkem. The solvents, such as anhydrous toluene, chloroform and acetonitrile from Aldrich were used as received. THF was used after distillation under sodium and benzophenone. Spectroscopic grade solvents from Aldrich were used for spectral measurements. 4-bromo-7-(4-formylbenzyl)-2,1,3-benzothiadiazole was synthesised according to literature[31].

Synthesis of 4-(3-Octylthien-2-yl)-N,N-dipphenylamine (2). Under argon, 4-(diphenylamino)phenylboronic acid (1.65 g, 4.63 mmol), 2-bromo-3-octylthiophene (1.16 g, 4.21 mmol), K_2CO_3 (700 mg, 5.05 mmol) and $Pd(PPh_3)_4$ (200 mg, 0.17 mmol) were dissolved in a degazed toluene/THF/water solution (30 mL, 20/7.5/2.5). The mixture was stirred overnight at 75°C before being poured into water. The organic phase was recovered with Et2O, washed with brine, dried on Na2SO4 and concentrated under reduced pressure. The crude oil was purified by chromatography on silica gel using *n*-hexane/CH_2Cl_2 2 : 1 to afford pale yellow oil **2** (1,67 g, 3.62 mmol, 86,0%). ^{1}H NMR (CD_2Cl_2, 200 MHz): δ = 7.33–7.96 (m, 16H), 2.66 (t, 2H, J = 7.8 Hz), 1.64–1.53 (m, 2H), 1.41–1.20 (m, 10H), 0.88 (t, 3H, J = 3 Hz). ^{13}C NMR (CD_2Cl_2, 50 MHz): 148.10, 147.52, 138.76, 138.09, 130.48, 130.09, 129.83, 129.17, 125.06, 124.63, 123.69, 123.60, 32.45, 31.60, 30.030, 29.95, 29.83, 29.20, 23.25, 14.55, HRMS (ESI): $[M + Na]^+$ = 439.23 (calcd. for $C_{30}H_{33}NS$: 439.23); Anal. Calcd for $C_{30}H_{33}NS$: C,81.96; H,7.57; N,3.19; S,7.29,. Found: C,81.66; H,7.67; N,3.22; S,7.47.

Synthesis of 4-(7-(5-(4-(diphenylamino)phenyl-4-octylthien-2-yl)benzo[c][1,2,5]thiadia-zol-4-yl)benzaldehyde (4). Under argon, **2** (200 mg, 0.45 mmol) was dissolved in distilled THF (8 mL) then *n*-BuLi (0.32 mL, 0.58 mmol) was added at −78°C. The solution was stirred for an hour at −50°C before adding a *n*-hexane solution of Me_3SnCl (0.73 mL, 0.72 μmol) at −78°C. The solution was allowed to reach room temperature and stirred for 2 hours. The reaction was quenched with water and the organic phase was extracted with *n*-hexane, dried with Na_2SO_4, filtered and concentrated under reduced pressure. The resulting oil **3** was engaged without any further purification in a Stille coupling with **1**. Under argon, solids **3**, **1** (174 mg, 0.55 mmol), Pd_2dba_3 (16 mg, 18 μmol) and P(*o*-tolyl)$_3$ (44 mg, 0.14 mmol) were dissolved in anhydrous toluene (8 mL) and refluxed for 24 hours. The mixture was then poured into HCl (1 M). The organic phase was extracted with Et_2O, washed with HCl (1 M), dried over Na_2SO_4 and concentrated under reduced pressure. The crude solid was purified by chromatography on silica gel using DCM/*n*-hexane 6 : 4 first then DCM as eluent to afford red solid **4**(270 mg, 0.40 mmol, 87%). ^{1}H NMR ($CDCl_3$, 200 MHz): δ = 10.11 (s, 1H), 8.19 (d, 2H, J = 8.4 Hz), 8.08 (s, 1H), 8.07 (d, 2H, J = 8.2 Hz), 7.96 (d, 1H, J = 7.6 Hz), 7.82 (d, 1H, J = 7.6 Hz), 7.42–7.26 (m, 6H), 7.19–7.03 (m, 8H), 2.77 (t, 2H, J = 7.8 Hz), 1.80–1.66 (m, 2H), 1.45–1.19 (m, 10H), 0.87 (t, 3H, J = 6.6 Hz); ^{13}C NMR ($CDCl_3$, 50 MHz): δ = 191.83, 153.68, 152.64, 147.42, 147.36, 143.23, 140.30, 139.46, 136.11, 135.632, 131.03, 130.50, 129.93, 129.81, 129.66, 129.33, 128.94, 127.84, 127.71, 124.74, 123.24, 122.87, 31.880, 31.04, 29.56, 29.42, 29.27, 28.97, 22.67, 14.13,; HRMS (ESI): $[M + Na]^+$ = 677.25 (calcd. for $C_{43}H_{39}N_3OS_2$: 677.25); Anal. Calcd for $C_{43}H_{39}N_3OS_2$: C, 76.18; H, 5.80; N, 6.20; S, 9.46. Found C, 76.07; H, 5.73; N, 6.17; S, 9.65.

Synthesis of RK1 dye. Under argon, **4** (134 mg, 0.18 mmol), cyanoacetic acid (78 mg, 0.90 mmol), were dissolved in a mixture of acetonitrile (6 mL) and chloroform (4 mL). A catalytic amount of piperidine was added and the solution was refluxed for 3 hours. Solvent was removed under reduced pressure and the solid dissolved in chloroform. The organic phase was washed with HCl solution (1.5 M), dried on Na_2SO_4 and concentrated. The crude solid was purified by chromatography on silica gel using DCM/MeOH/Acetic acid 90 : 5 : 5 as eluent to afford **RK1** as red solid 5 (128 mg, 0.16 mmol, 87%). ^{1}H NMR ($CDCl_3$, 200 MHz): δ = 8.36 (s, 1H), 16 (s, 4H), 8.06 (s, 1H), 7,91 (d, 1H, J = 7.4 Hz), 7.79 (d, 1H, J = 7.6 Hz), 7.40–7.26 (m, 6H), 7.18–7.03 (m, 8H), 2.74 (t, 2H, J = 7.8 Hz), 1.78–1.66 (m, 2H), 1.42–1.21 (m, 10H), 0.87 (t, 3H, J = 6.6 Hz); ^{13}C NMR (THF-d_8, 50 MHz): δ = 163.57, 154.40, 153.76, 153.38, 148.32, 148.29, 142.22, 140.94, 139.85, 137.13, 132.27, 131.70, 131.65, 130.84, 130.39, 130.28, 129.99, 129.53, 128.78, 128.15, 125.44, 125.36, 123.95, 123.47, 116.17, 104.35, 32.681, 31.75, 30.31, 30.22, 30.09, 29.61, 23.38, 14.29,; HRMS (Q-TOF): $[M - H]^-$ = 743.25145 (calcd. for $C_{46}H_{39}N_4O_2S_2$: 743.2519), $[M\text{-}CO_2H]^-$ = 699.26162 (calcd. for $C_{45}H_{39}N_4S_2$: 699.2628); Anal. Calcd for $C_{46}H_{40}N_4O_2S_2$: C, 74.16; H, 5.41; N, 7.52; S, 8.61. Found: CC, 73.87; H, 5.51; N, 7.41; S, 8.89.

Optical and electrochemical characterizations. UV-vis absorption spectra were recorded in solution on a Perkin-Elmer Lambda 2 spectrometer (wavelength range: 180–820 nm; resolution: 2 nm). Electrochemical studies of the synthesized molecules were carried out in a one compartment, three-electrode electrochemical cell equipped with a flat platinum working electrode (7 mm^2), a Pt wire counter electrode, and a Ag wire pseudo-reference electrode, whose potential was checked using the Fc/Fc^+ couple as an internal standard. The electrolyte consisted of 0.1 M tetrabutylammonium tetrafluoroborate (Bu_4NBF_4) solution in dichloromethane containing 2×10^{-3} M of the dye. The experiments were carried out in a glove box.

Modelling. The density functional theory (DFT) calculations were performed on the two organic sensitizers by using the Amsterdam Density Functional package (ADF 2010.01) [ADF2010, SCM, Theoretical Chemistry, Vrije Universiteit, The Netherlands Amsterdam, http://www.scm.com (scientific computing and modelling accessed 21-01-2014)][32,33]. The structures of the dyes have been fully optimized at a GGA level using the Perdew-Burke-Ernzerhof (PBE) functional and triple zeta plus 2 polarization Slater functions (TZ2P set in ADF) basis sets for all atoms, with 1 s orbitals frozen for C, N and O atoms. On these optimized geometries, B3LYP hybrid functional calculations with TZ2P all electron basis sets were then performed to yield more reliable frontier orbital energies. Acetonitrile solvent was taken into account using a polarizable continuum model (COSMO in ADF)[34] for all geometry optimizations and B3LYP single point calculations. Orbitals were drawn using the graphical interface of ADF (ADF-GUI).

Solar cell fabrication and characterization. For optimized DSC devices employing acetonitrile electrolyte, photoanodes consisted of a 13 μm layer of mesoporous TiO_2 and a 4 μm scatter layer were prepared. Prior to the deposition of the TiO_2 paste the conducting glass substrates were immersed in a solution of $TiCl_4$ (40 mM) at 70°C for 30 min, washed with water and ethanol and then dried. The TiO_2 nanoparticle paste was deposited onto a conducting glass substrate (NSG glass with 8 Ω cm^{-2} resistance) using the screen printing technique. The TiO_2 electrodes were gradually heated under airflow at 325°C for 5 min, 375°C for 5 min, 450°C for 15 min and 500°C for 15 min. The heated TiO_2 electrodes were immersed again in a solution of $TiCl_4$ (40 mM) at 70°C for 30 min and then washed with water and ethanol. The electrodes were heated again at 500°C for 30 min and cooled before sensitization. In order to reduce scattered light from the edge of the glass electrodes of the dyed TiO_2 layer, a light shading mask was used on the DSCs, so the active area of DSCs was fixed to 0.16 cm^2. The counter electrode was made by spreading a 5 mM solution of H_2PtCl_6 in isopropyl alcohol onto a conducting glass substrate (TEC15, Pilkington) with a small hole to allow the introduction of the liquid electrolyte using vacuum, followed by heating at 390°C for 15 min. TiO_2 films were dipped overnight in the corresponding dye solution. The sensitized electrodes were washed with ethanol and dried under air. Finally, the working and counter electrodes were sandwiched together using a thin thermoplastic (Surlyn) frame that melts at 100°C. The volatile electrolyte used consisted of 0.5 M 1-butyl-3- methylimidazolium iodide (BMII), 0.1 M lithium iodide, 0.05 M iodine and 0.5 M tert-butylpyridine in acetonitrile. The non-volatile electrolyte used consisted of (molar ratio) DMII (12), EMII (12), EMITCB (16), I_2 (1.67), n Butyl benzimidazole (3.33), Guanidinium thiocyanate (0.67).

Charge extraction and transient photovoltage measurements. For charge extraction white light from a series of LEDs was used as the light source. When the LEDs are turned off, the cell is immediately short circuited and the charge is extracted allowing the electron density in the cells to be calculated. By changing the intensity of the LEDs, the electron density can be estimated as a function of cell voltage. In transient photovoltage measurements, in addition to the white light applied by the LEDS, a diode pulse (660 nm, 10 mW) is applied to the sample inducing a change of 2–3 mV within the cell. The resulting photovoltage decay transients are collected and the τ values are determined by fitting the data to the equation $\exp(-t/\tau)$.

1. Hardin, B. E., Snaith, H. J. & McGehee, M. D. The renaissance of dye-sensitized solar cells. *Nature Photon.* **6**, 162–169 (2012).
2. Boschloo, G. & Hagfeldt, A. Characteristics of the iodide/triiodide redox mediator in dye-sensitized solar cells. *Acc. Chem. Res.* **42**, 1819–1826 (2009).
3. O'Regan, B. & Grätzel, M. A low-cost, high-efficiency solar-cell based on dye-sensitized colloidal TiO2 films. *Nature* **353**, 737–740 (1991).
4. Grätzel, M. Recent advances in sensitized mesoscopic solar cells. *Acc. Chem. Res.* **42**, 1788–1798 (2009).
5. Ardo, S. & Meyer, G. J. Photodriven heterogenous charge transfer with transition metal compounds anchored to TiO2 semiconductor surfaces. *Chem. Rev.* **38**, 115–164 (2009).
6. Hagfeldt, A., Boschloo, G., Sun, L. C., Kloo, L. & Pettersson, H. Dye-sensitized solar cells. *Chem. Rev.* **110**, 6595–6663 (2010).
7. Yu, Q. *et al.* High-Efficiency dye-sensitized solar cells: the influence of lithium ions on exciton dissociation, charge recombination, and surface states. *ACS Nano* **4**, 6032–6038 (2010).
8. Nazeeruddin, M. K. *et al.* Conversion of light to electricity by *cis-X*2bis (2,2′-bipyridyl-4,4′-dicarboxylate)ruthenium(II) charge-transfer sensitizers (X = Cl–, Br–, I–, CN–, and SCN–) on nanocrystalline titanium dioxide electrodes. *J. Am. Chem. Soc.* **115**, 6382–6390 (1993).
9. Gao, F. *et al.* Enhance the optical absorptivity of nanocrystalline TiO_2 film with high molar extinction coefficient ruthenium sensitizers for high performance dye-sensitized solar cells. *J. Am. Chem. Soc.* **130**, 10720–10728 (2008).
10. Choi, S.-H. *et al.* Amorphous zinc stannate (Zn_2SnO_4) nanofibers networks as photoelectrodes for organic dye-sensitized solar cells. *Adv. Funct. Mater.* **23**, 3146–3155 (2013).
11. Katoh, R. *et al.* Highly stable sensitizer dyes for dye-sensitized solar cells: role of the oligothiophene moiety. *Energy Environ. Sci.* **2**, 542–546 (2009).
12. Wang, Z.-S. *et al.* Molecular Design of Coumarin Dyes for Stable and Efficient Organic Dye-Sensitized Solar Cells. *J. Phys. Chem. C.* **112**, 17011–17017 (2008).
13. Mishra, A., Fischer, M. K. R. & Bäuerle, P. Metal-free organic dyes for dye-sensitized solar cells: from structure: property relationships to design rules. *Angew. Chem. Int. Ed.* **48**, 2474–2499 (2009).
14. Yum, J.-H. *et al.* Blue-coloured highly efficient dye-sensitized solar cells by implementing the diketopyrrolopyrrole chromophore. *Sci. Rep.* **3**, 2446–2453 (2013).
15. Zhang, M. *et al.* Design of high-efficiency organic dyes for titania solar cells based on the chromophoric core of cyclopentadithiophene-benzothiadiazole. *Energy Environ. Sci.* **6**, 2944–2949 (2013).
16. Wu, Y. & Zhou, W. Organic sensitizers from D–π–A to D–A–π–A: effect of the internal electron-withdrawing units on molecular absorption, energy levels and photovoltaic performances. *Chem. Soc. Rev.* **42**, 2039–2058 (2013).
17. Zeng, W. *et al.* Efficient dye-sensitized solar cells with an organic photosensitizer featuring orderly conjugated ethylenedioxythiophene and dithienosilole blocks. *Chem. Mater.* **22**, 1915–1925 (2010).
18. Bessho, T., Zakeeruddin, S. M., Yeh, C.-Y., Diau, E. W.-G. & Gratzel, M. Highly efficient mesoscopic dye-sensitized solar cells based on donor–acceptor-substituted porphyrins. *Angew. Chem.* **122**, 6796–6799 (2010).
19. Yella, A. *et al.* Porphyrin-Sensitized Solar Cells with Cobalt (II/III)–Based Redox Electrolyte Exceed 12 Percent Efficiency. *Science* **334**, 629–634 (2011).
20. Kurotobi, K. *et al.* Highly asymmetrical porphyrins with enhanced push–pull character for dye-sensitized solar cells. *Chem. Eur. J.,* dx.doi.org/10.1002/chem.201303460 (2013).
21. Kim, J.-J. *et al.* Polymer gel electrolyte to achieve ≥6% power conversion efficiency with a novel organic dye incorporating a low-band- gap chromophore. *J. Mat. Chem.* **18**, 5223–5229 (2008)
22. Zhu, W. *et al.* Organic D-A-π-A solar cell sensitizers with improved stability and spectral response. *Adv. Funct. Mater.* **21**, 756–763 (2011).
23. Haid, S. *et al.* Significant Improvement of Dye-Sensitized Solar Cell Performance by Small Structural Modification in π-Conjugated Donor–Acceptor Dyes. *Adv. Funct. Mater.* **22**, 1291–1302 (2012).
24. Clifford, J. N., Palomares, E., Nazeeruddin, S., Grätzel, M. & Durrant, J. R. Dye dependent regeneration dynamics in dye sensitized nanocrystalline solar cells: evidence for the formation of a ruthenium bipyridyl cation/iodine intermediate. *J. Phys. Chem. C* **111**, 6561–6567 (2007).
25. Yum, J. H. *et al.* Effect of coadsorbent on the photovoltaic performance of squaraine sensitized nanocrystalline solar cells. *Nanotechnology* **19**, 424005 (2008).
26. Clifford, J. N., Planells, M. & Palomares, E. Advances in high efficiency dye sensitized solar cells based on Ru(II) free sensitizers and a liquid redox electrolyte. *J. Mater. Chem.* **22**, 24195–24201 (2012).
27. Zakeeruddin, S. M. & Grätzel, M. Solvent-free ionic liquid electrolytes for mesoscopic dye-sensitized solar cells. *Adv. Funct. Mater.* **19**, 2187–2202 (2009).
28. Gorlov, M. & Kloo, L. Ionic liquid electrolytes for dye-sensitized solar cells. *Dalton Trans.* 2655–2666 (2008).
29. Zhang, Z., Ito, S., Moser, J.-E., Zakeeruddin, S. M. & Grätzel, M. Influence of iodide concentration on the efficiency and stability of dye-sensitized solar cell containing non-volatile electrolyte. *Chem. Phys. Chem.* **10**, 1834–1838 (2009).
30. Popov, A. I. & Swensen, R. F. Studies on the chemistry of halogens abd of polyhalides V. Spectroscophotometric study of polyhalogen complexes in acetronitrile and in ethylene dichloride. *J. Am. Chem. Soc.* **77**, 3724–3726 (1955).
31. Sandanayaka, A. S. D. *et al.* Photoinduced charge separation and charge recombination in the [60]fullerene−diphenylbenzothiadiazole−triphenylamine triad: role of diphenylbenzothia-diazole as bridge. *J. Phys. Chem. B.* **109**, 22502 (2005).
32. te Velde, G. *et al.* Chemistry with ADF. *J. Comput. Chem.* **22**, 931–967 (2001).
33. Fonseca Guerra, C., Snijders, J. G., te Velde, G. & Baerends, E. J. Towards an order-N DFT method. *Theor. Chem. Acc.* **99**, 391–403 (1998).
34. Pye, C. C. & Ziegler, T. An implementation of the conductor-like screening model of solvation within the Amsterdam density functional package. *Theor. Chem. Acc.* **101**, 396–408 (1999).

Acknowledgments

Gaelle Berthoux and Yann Kervella are acknowledged for their assistance in the synthesis of some of the intermediates. Dr Pascale Maldivi is acknowledged for the density functional theory (DFT) calculations. Authors acknowledge the European Union Research Executive Agency for funding through the Adios-Ru research project. This project is funded by the European Union Research Executive Agency (contract 315131) on the Research for SMEs programme. Emilio Palomares would like to thank ICIQ and ICREA for economic support.

Author contributions

D.J. synthesized and characterized the dye. F.O., S.N., L.P. and J.N.C. carried out the fabrication and the optimisation of the solar cells and designed and analysed the experiments. L.P. and J.N.C. performed the photo physical characterization of the devices. F.O. and S.N. performed the lifetime measurements and stability tests of the solar cells. J.C. contributed to the optimization of the synthesis of the dye. R.D. designed the dye, R.D. and E.P. designed the experiments, contributed to the analysis of the data and wrote the paper. All the authors revised the manuscript.

Additional information

Competing financial interests: RD and DJ are employees of CEA which holds a patent on this technology, JC is the CEO of Kaironkem which holds a license and commercializes this product. SN and FO are employees of Solaronix which distributes the product. Therefore these authors declare competing interests as defined by Nature Publishing Group, or other interests that might be perceived to influence the results and/or discussion reported in this article.

How to cite this article: Joly, D. *et al.* A Robust Organic Dye for Dye Sensitized Solar Cells Based on Iodine/Iodide Electrolytes Combining High Efficiency and Outstanding Stability. *Sci. Rep.* **4**, 4033; DOI:10.1038/srep04033 (2014).